Powder Metallurgy and Metal Ceramics, Vol. 46, Nos. 7-8, 2007

PHYSICOCHEMICAL MATERIALS RESEARCH

PHASE RELATIONS IN THE Al–Ir–Os SYSTEM IN THE RANGE UP TO 70 at.% Al

S. O. Katrych, V. M. Petyukh, A. A. Bondar, and W. Steurer

UDC 621.762

For alloys in the range Os–$OsAl_2$–$IrAl_{2.7}$–Ir, as-cast and annealed at 1400°C (Os–OsAl– IrAl–Ir) and 1250°C (OsAl–$OsAl_2$–$IrAl_{2.7}$–IrAl), phase equilibria are studied by powder x-ray diffraction (PXRD), differential thermal analysis (DTA), scanning electron microscopy (SEM) and energy-dispersive x-ray spectroscopy (EDX). Between isostructural aluminides OsAl and IrAl there exists a continuous solid solution (Os,Ir)Al. Other unary and binary phases form terminal solid solutions: (Os), (Ir), ($OsAl_2$), and ($IrAl_{2.7}$).

Keywords: *intermetallics, x-ray diffraction, high-temperature alloys, differential thermal analysis.*

INTRODUCTION

The Al–Ir–Os system is of interest due to potential applications of its alloys or compounds as coatings on some high-temperature materials as proposed for the Al–Ir alloys [1]. This ternary system has not yet been studied, and our work is focused on obtaining data on phase equilibria at melting (solidification) temperatures and at 1400°C (from 0 to ~50 at.% Al) or 1250°C (~50 to ~70 at.% Al). For the Al–Os binary system, no phase diagram is available. Only crystallographic data of its binary compounds have been reported in [2] (Table 1). For the Al–Ir phase diagram, there are two its versions at the Al content from 0 to 70 at.%, with congruent and incongruent melting of the $IrAl_{2.7}$ phase, as reported in [3] and [1], respectively. Phases based on Ir and IrAl form a eutectic at 2058°C (the temperature was estimated by calculation) and 30 at.% Al [1, 3]. The Ir–Os phase diagram was taken from [2, 4]. The Os-rich (Ir) phase is formed in the peritectic reaction l_p + (Os) → (Ir) at 2660°C.

EXPERIMENTAL

Six samples, about 1 g each, were studied in the composition range from 0 to 70 at.% Al. Four of them were produced in Ar (99.998 wt.% Ar) from Al-wire (99.9 wt.% Al, Alfa Asear) and pellets of pressed Ir and Os (99.9 wt.% purities, Alfa Asear) using arc-melting (MAM-1, Johanna Otto GmbH). The alloys were melted in such a way that at first Os–Ir compacts were melted and then the melt dissolved the Al-wire. Two samples, one with 70 and the other with 52 at.% Al, were prepared from the $Al_{65}Ir_{17.5}Os_{17.5}$ and $Al_{42.5}Ir_{20.5}Os_{37}$ prealloys, respectively, mixed with Al cuts. The total weight loss of the as-prepared alloys was checked to be less than ~1.5 at.% and nominal compositions were adopted. The alloy compositions are shown in Figs. 1 and 2.

Laboratory for Solid State Physics, ETH, Zurich. Institute for Problems of Materials Science, National Academy of Science of Ukraine, Kiev. Laboratory of Crystallography, Department of Materials, ETH, Zurich. Translated from Poroshkovaya Metallurgiya, Vol. 46, No. 7–8 (456), pp. 59–66, 2007. Original article submitted October 30, 2006.

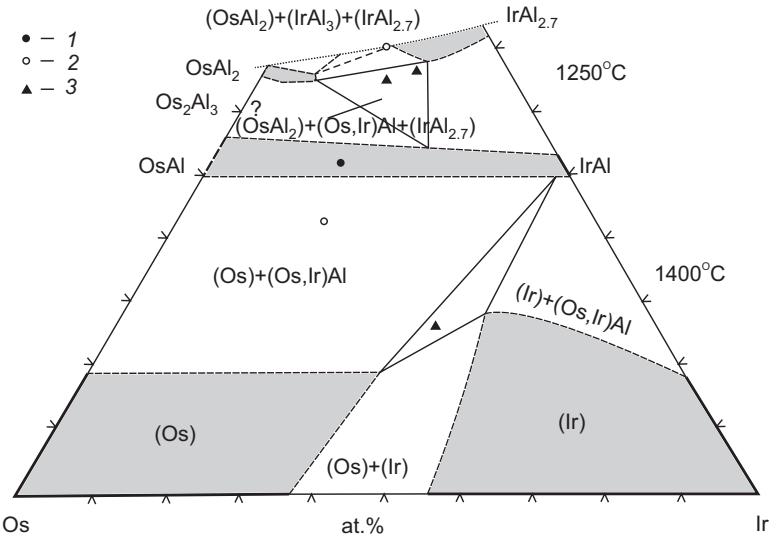

Fig. 1. Partial isothermal sections of the Al–Ir–Os system at 1400ºC (to ~50 at.% Al) and at 1250°C (from ~50 to ~70 at.% Al). Compositions of studied samples are shown as follows: (*1*) single-phase, (*2*) two-phase, (*3*) three- phase

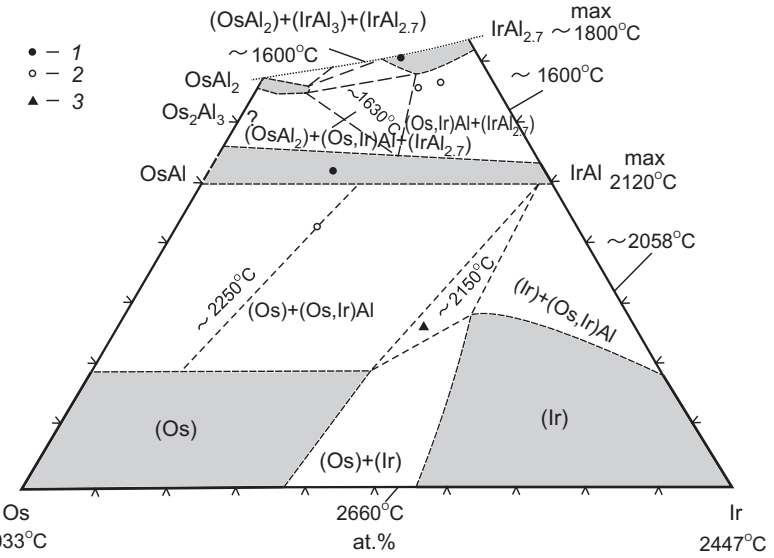

Fig. 2. Partial solidus surface projection of the Al–Ir–Os system for the range from 0 to ~70 at.% Al. Compositions of studied samples: (*1*) single-phase, (*2*) two-phase, (*3*) three-phase

All the alloys were annealed in a high-vacuum resistance furnace followed by cooling by jetting in cold Ar into the furnace chamber (MOV 064, Pfeiffer Vakuum Anlagebau GmbH). The samples were subjected to metallographic examination, PXRD (STOE diffractometer, Cu-K_{α_1} radiation), and DTA. The latter was carried out using a device equipped with W/W-20Re string thermocouples designed by Kocherzhinskii et al. [5, 6] under He of high purity at heating and cooling rates of about 40 °C/min. Crucibles were of Al_2O_3 and Y_2O_3. The higher temperature limit of the device was about 2250°C, more details are reported elsewhere [7]. The compositions of phases were EDX-checked at 15–30 kV accelerating voltage using a LEO 1530 analyzer and the VOYAGER software.

RESULTS AND DISCUSSION

No unknown phase was revealed by PXRD (Fig. 3, Table 2). Results of the microstructural examination, obtained on both as-cast and annealed samples, agree with the PXRD data. The microstructure of the as-cast $Al_{26}Ir_{44}Os_{30}$ sample illustrates that the (Os) phase crystallizes as the primary one (the large brightest grains in Fig. 4a, b). The grains of this phase are bordered with (Ir), which corresponds to the monovariant peritectic reaction L + (Os) → (Ir). Such a peritectic reaction is present in the binary Ir–Os system. The irregular phase distribution was also observed in some part of the sample as a result of phase segregation by density. In Fig. 4b, the left side of micrographs predominantly shows the (Os) phase and the right side shows more of (Ir). The crystallization of the last portion of the melt has a microstructure consistent with the invariant eutectic reaction $L_E \rightarrow$ (Ir) + (Os) + (Ir, Os)Al (Fig. 4c), while the DTA melting point obtained, 2150°C (Table 2), is in disagreement with the binary eutectic temperature calculated in [3] as 2058°C. The micrographs of this sample annealed at 1400°C for 50 h show the same three phases, differing from the as-cast one by precipitates in the (Os) and (Ir) grains.

TABLE 1. Crystal Structure Data and Lattice Parameters for the Relevant Al–Ir–Os Phases

Phase	Temperature range of stability, °C	Pearson symbol	Space	Prototype	Lattice parameters	
					a, *c*, pm	Comments
(Ir)	<2660	*cF*4	$Fm\bar{3}m$	Cu	*a* = 383.92	Pure [2]
					a = 383.8	Ir–20.1 at.% Al [1]
					a = 384.93	Ir–31.2 at.% Os [4]
					a = 382.67	$Al_{28}Ir_{50}Os_{22}$ (this study)
(Os)	<3033	*hP*2	$P6_3/mmc$	Mg	*a* = 273.41 *c* = 431.98	Pure [2]
					a = 273.61 *c* = 434.17	Os–35 at.% Ir [4]
					a = 273.37(4) *c* = 432.2(1)	$Al_{18}Ir_4Os_{78}$ (this study)
					a = 272.76(4) *c* = 433.34(8)	$Al_{18.5}Ir_{40}Os_{41.5}$ (this study)
IrAl	<2120	*cP*2	$Pm\bar{3}m$	CsCl	*a* = 298.4	[1][1]
					a = 297.8	[1][2]
OsAl	?				*a* = 300.1(1)	[8][3]
					a = 300.5(9)	[9][3]
(Os, Ir)Al	?				*a* = 299.25(5)	$Al_{45.5}Ir_{22.5}Os_{32}$ (this study)[1]
(β)					*a* = 298.64(6)	$Al_{54.5}Ir_{25.5}Os_{20}$ (this study)[2]
$IrAl_{2.7}$	<~1800	*cP*32	$Pm\bar{3}n$		*a* = 768.5	[10][1]
(Al_5Ir_2)					*a* = 766.0	[10][2]
					a = 767.89(3)	Ir–73 at.% Al [11]
					a = 768.76(3)	$Al_{67.8}Ir_{21.5}Os_{10.7}$ (this study)
Os_2Al_3	?	*tI*10	*I*4/*mmm*		*a* = 310.6(1) *c* = 1418.4(2)	[10][1]
$OsAl_2$	?	*tI*6	*I*4/*mmm*	$MoSi_2$	*a* = 316.2(3) *c* = 830.2(5)	[10][1]
					a = 316.41(1) *c* = 829.53(3)	$Al_{65}Ir_8Os_{27}$ (this study)

[1] Al-lean composition. [2] Al-rich composition. [3] Al-stoichiometric composition.

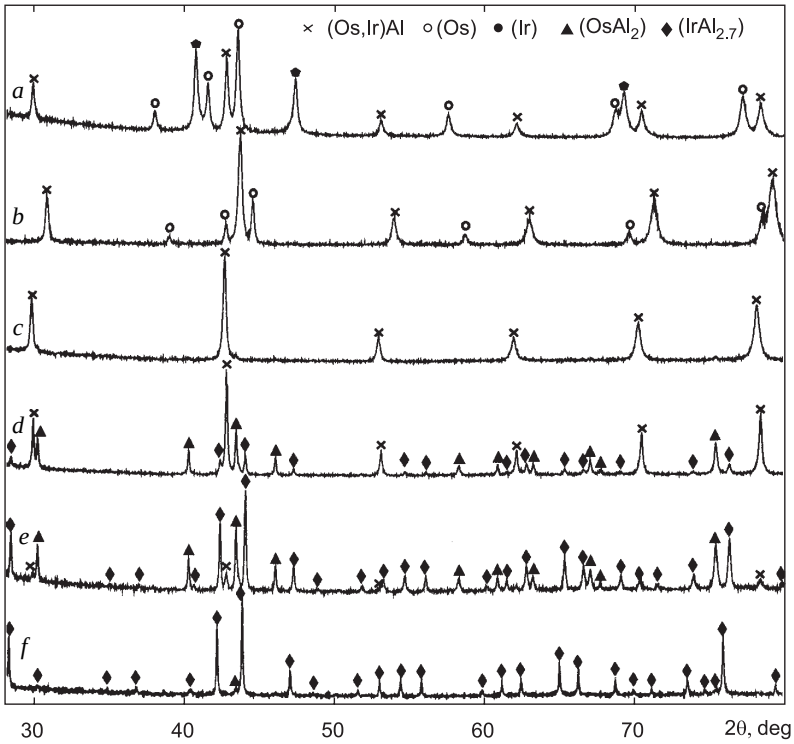

Fig. 3. Powder x-ray diffraction patterns (Cu-K_{α_1}): (*a*) $Al_{26}Ir_{44}Os_{30}$ annealed at 1400°C for 50 h; (*b*) $Al_{42.5}Ir_{20.5}Os_{37}$ annealed at 1400°C for 50 h; (*c*) $Al_{52}Ir_{17}Os_{31}$ annealed at 1250°C for 5 h; (*d*) $Al_{65}Ir_{17.5}Os_{17.5}$ annealed at 1250°C for 5 h; (*e*) $Al_{66.5}Ir_{21}Os_{12.5}$ annealed at 1250°C for 5 h; (*f*) $Al_{70}Ir_{15}Os_{15}$ annealed at 1250°C for 6 h

TABLE 2. PXRD and DTA Data for the Al–Ir–Os Alloys

Sample	Phase constituents	DTA temperature, °C		
		Onset point of melting	Completion of melting	Onset point of solidification
$Al_{26}Ir_{44}Os_{30}$, as-cast	(Os) + (Ir) + (Os, Ir)Al	~2250		
The same annealed at 1400°C for 50 h	Same			
$Al_{42.5}Ir_{20.5}Os_{37}$, as-cast	(Os) + (Ir) + (Os, Ir)Al	2150		
The same annealed at 1400°C for 50 h	Same			
$Al_{52}Ir_{17}Os_{31}$, as-cast	(Os, Ir)Al	1760–1795[1]	1820	1830
The same annealed at 1250°C for 5 h	Same			
$Al_{65}Ir_{17.5}Os_{17.5}$, as-cast	(Os, Ir)Al + ($IrAl_{2.7}$)	1632	1648	1576
The same annealed at 1250°C for 5 h	(Os, Ir)Al + ($IrAl_{2.7}$) + ($OsAl_2$)			
$Al_{66.5}Ir_{21}Os_{12.5}$, as-cast	(Os, Ir)Al + ($IrAl_{2.7}$)	1634	1662	1650
The same annealed at 1250°C for 5 h	(Os, Ir)Al + ($IrAl_{2.7}$) + ($OsAl_2$)			
$Al_{70}Ir_{15}Os_{15}$, as-cast	($IrAl_{2.7}$)	1610 (1655)	1678	1603 (1580)[2]
The same annealed at 1250°C for 5 h	($IrAl_{2.7}$) + ($OsAl_2$)			

[1] Illegible beginning. [2] Two effects on both heating and cooling curves.

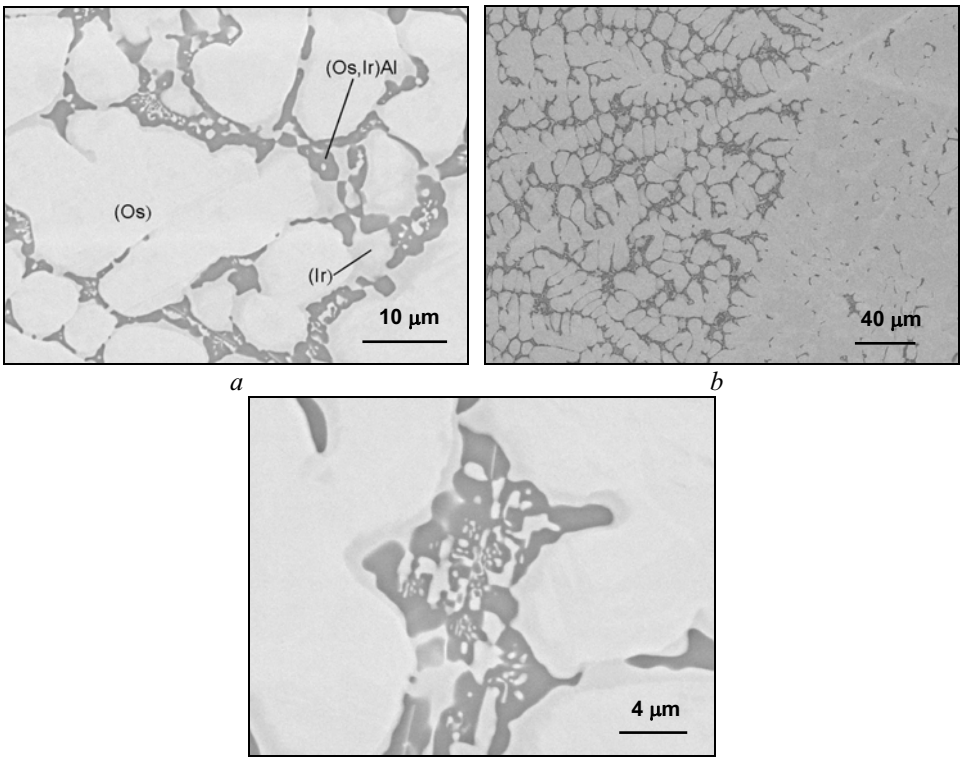

a *b*

c

Fig. 4. SEM micrographs (backscattered electron images) of as-cast $Al_{26}Ir_{44}Os_{30}$ alloy, (Os) + (Ir) + (Os, Ir)Al

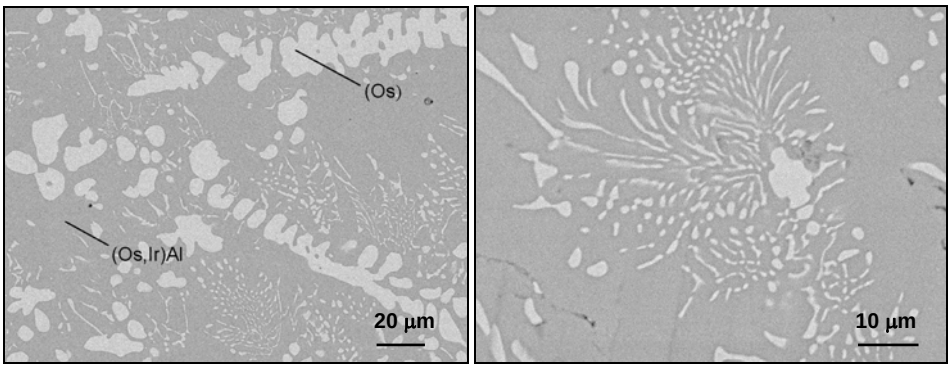

a *b*

Fig. 5. SEM micrographs (backscattered electron images) of as-cast $Al_{42.5}Ir_{20.5}Os_{37}$ alloy, (Os) + (Os, Ir)Al

The microstructure of the as-cast $Al_{42.5}Ir_{20.5}Os_{37}$ sample shows two phases, the (Os) phase and the solid solution (Os, Ir)Al (Fig. 5). One can see the (Os) phase, crystallized as primary grains, and a two-phase eutectic component. The (Os) phase composition was found to be ~19 at.% Al and ~3 at.% Ir, which indicates that the homogeneity field of (Os) is ~20 at.% Al or higher in the binary Al–Os system. The moderate quantity of the primary (Os) phase and the overall composition of the eutectic determined by EPMA as $Al_{41}Ir_{25}Os_{34}$ show that the monovariant line of joint crystallization of both phases is located close to the sample composition (not excepting the existence of the quasibinary eutectic reaction $L_e \rightarrow$ (Os, Ir)Al + (Os)). After annealing at 1400°C for 50 h, the microstructure of this alloy remains similar to the as-cast state.

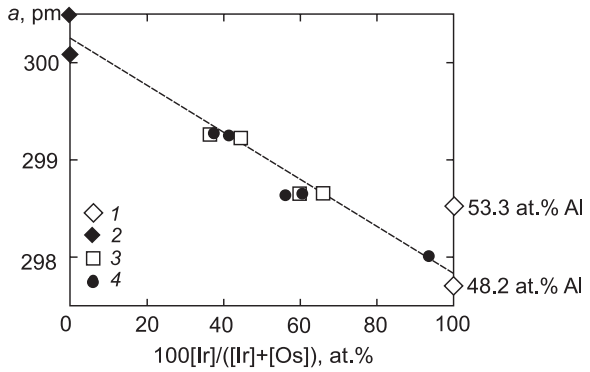

Fig. 6. Lattice parameter *a* for the (Os, Ir)Al phase vs. composition: (*1*) data from [1] for the Al–Ir binary alloy at Al-lean and Al-rich composition; (*2*) data from [8] and [9] for the Al–Os binary alloy at stoichiometric composition; (*3*) and (*4*) the present data for Al–Ir–Os ternary alloys, as-cast and annealed (at 1250 and 1400°C), respectively

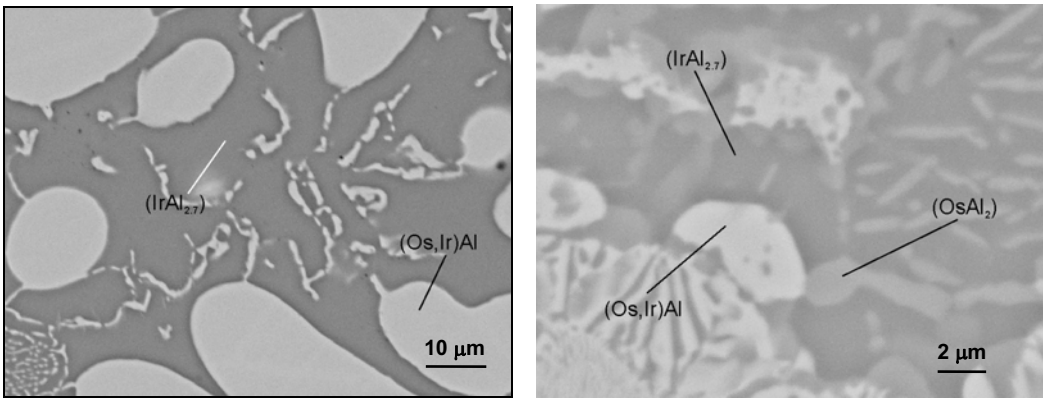

a *b*

Fig. 7. SEM micrographs (backscattered electron images) of $Al_{65}Ir_{17.5}Os_{17.5}$ alloy: (*a*) as-cast; (*b*) annealed at 1250°C for 5 h

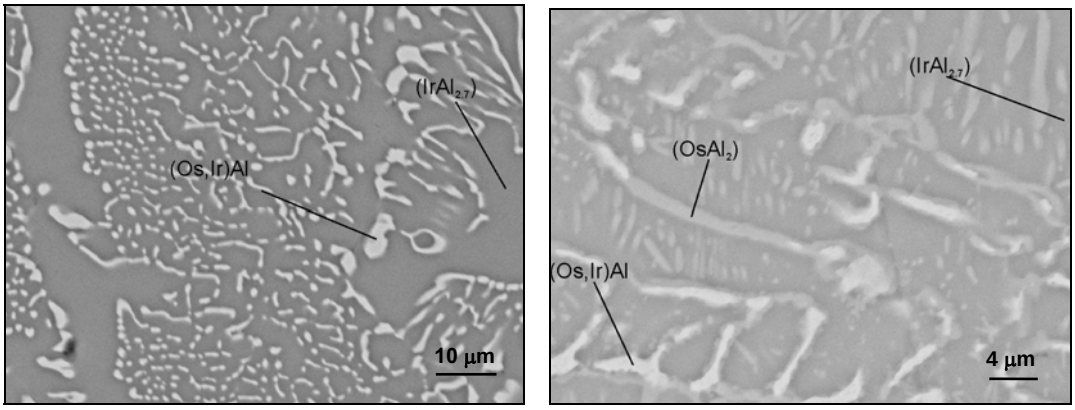

a *b*

Fig. 8. SEM micrographs (backscattered electron images) of $Al_{66.5}Ir_{21}Os_{12.5}$ alloy: (*a*) as-cast; (*b*) annealed at 1250°C for 5 h

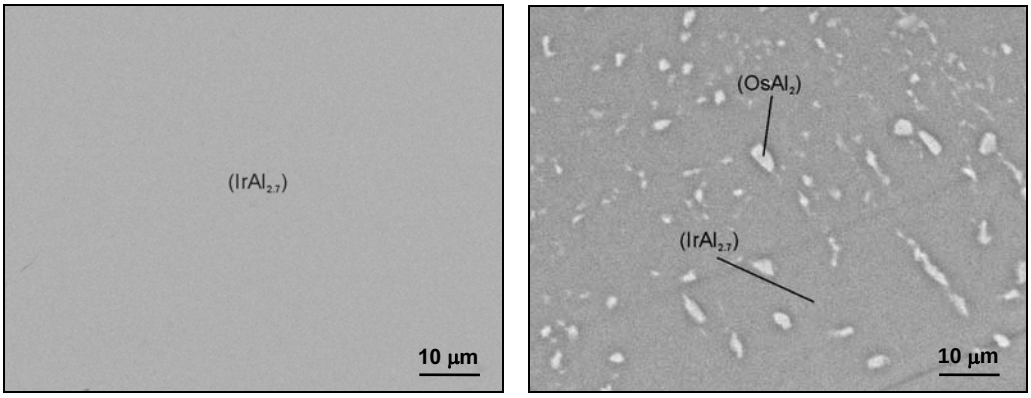

a *b*

Fig. 9. SEM micrographs (backscattered electron images) of $Al_{70}Ir_{15}Os_{15}$ alloy: (*a*) as-cast; (*b*) annealed at 1250°C for 5 h

The $Al_{52}Ir_{17}Os_{31}$ sample is single-phase in both states, as-cast and annealed at 1250°C for 5 h (Fig. 3), which corresponds to the solid solution between OsAl and IrAl. An analysis of the dependence of the lattice parameter on the composition confirms the formation of the (Os, Ir)Al continuous solid solution (Fig. 6). Based on the DTA melting temperature varying from 1760 to ~1800°C (the beginning of arrest was illegible and the sample surface was somewhat fused), the alloy composition is richer in Al.

Both as-cast and annealed samples of the $Al_{65}Ir_{17.5}Os_{17.5}$ and $Al_{66.5}Ir_{21}Os_{12.5}$ alloys are within the same phase fields (Figs. 7 and 8). The as-cast samples are two-phase (Os, Ir)Al + ($IrAl_{2.7}$) and contain the eutectic of these phases (Figs. 7a and 8a). The eutectic composition is close to the $Al_{66.5}Ir_{21}Os_{12.5}$ alloy (it is not known whether it is invariant quasibinary or monovariant), and another alloy, $Al_{65}Ir_{17.5}Os_{17.5}$, is in the field of primary solidification of (Os, Ir)Al. After annealing at 1250°C for 5 h, the $OsAl_2$-based phase precipitated as gray lamellae (Figs. 7b and 8b). This is associated with the reduction of the homogeneity field of the terminal solid solution ($IrAl_{2.75}$) with the temperature falling from melting at ~1600°C to the annealing temperature at 1250°C. This was confirmed by the $Al_{70}Ir_{15}Os_{15}$ alloy that is single-phase in as-cast state and contains the ($OsAl_2$) precipitate after annealing (Fig. 9a, b). It seems that the ternary terminal solid solution ($IrAl_{2.75}$) melts congruently as it is in the Al–Ir binary phase diagram [1].

CONCLUSION

All the results are combined in the partial isothermal sections (Fig. 1) at 1250 and 1400°C and in the partial solidus surface projection (Fig. 2). In spite of the tentative nature of these phase diagrams for the ternary system, the main peculiarities become clear. As seen, the mutual solid solubility in the (Os) and (Ir) phases is high. The OsAl and IrAl intermetallics form a continuous solid solution, (Os, Ir)Al. The $IrAl_{2.7}$ phase dissolves not less than 15 at.% Os, and $OsAl_2$ ranges to approximately 8 at.% Ir at 1250°C.

ACKNOWLEDGEMENT

S.K. and W.S. gratefully acknowledge financial support under grant SNF 200020-105158.

REFERENCES

1. P. J. Hill, L. A. Cornish, and M. J. Witcomb, “Constitution and hardness of the Al–Ir system,” *J. Alloys Comp.*, **280**, 240–250 (1998).

2. T. B. Massalski, P. R. Subramanian, H. Okomoto, and L. Kasprzak (Eds.), Binary *Alloy Phase Diagrams*, 3 vols., Metals Park, ASM, Ohio (1990), p. 3589.
3. K. M. Axler, E. M. Foltyn, D. E. Peterson, and W. B. Hutchinson, "Phase investigation of the Al–Ir system," *J. Less-Common. Met.*, **156**, 213–219 (1989).
4. H. Okamoto, "The Ir–Os (Iridium–Osmium) system," *J. Phase Equi.*, **15,** No. 1, 55–57 (1994).
5. Ju. A. Kocherzhinsky, "Differential thermocouple up to 2450°C and thermographic investigations of refractory silicides," in: *Thermal Analysis: Proceeding of Third ICTA (Davos)*, Vol. 1, Birkhäuser Verlag, Basel (1971), pp. 549–559.
6. Yu. A. Kocherzhinskii, E. A. Shishkin, and V. I. Vasilenko, "An apparatus for DTA with a thermocouple sensor to 2200°C," in: *Phase Diagrams for Metal Systems* [in Russian], Nauka, Moscow (1971), pp. 245–249.
7. T. Ya. Velikanova, A. A. Bondar, and A. V. Grytsiv, "The chromium–nickel–carbon phase diagram," *J. Phase Equilibria*, **20**, No. 2, 125–147 (1999).
8. L. E. Edshammar, "The Crystal Structures of Os_2Al_3 and $OsAl_2$," *Acta Chem. Scand.*, **19**, 871–874 (1965).
9. P. Esslinger and K. Schubert, "Zur Systematik der Strukturfamilie des NiAs," *Z. Metallkunde*, **48**, 126–134 (1957).
10. P. Villars and L. D. Calvert, *Pearson Handbook of Crystallographic Data for Intermetallic Phases*, 2nd ed., 4 vols., Metals Park, ASM Int., Ohio (1991).
11. Yu. Grin, K. Peters, U. Bukhardt, et al., "The crystal structure of the binary iridium–aluminum $IrAl_{2.75}$ and rhodium–aluminum $RhAl_{2.63}$ phase," *Zeit. f. Krist.*, **212**, 439–444 (1997).